RPE | Radiation Physics & Engineering
An International Peer-Reviewed Journal
Published by K.N. Toosi University of Technology
http://rpe.kntu.ac.ir
Research Article

Radiation Physics and Engineering 2021; 2(4):29–37
https://doi.org/10.22034/RPE.2022.315654.1045

Assessment of granite-kaolin composite bricks as storage barrier facility for liquid radioactive waste

E.O. Echeweozo[a,b,*], A.D Asiegbu[b,*], E.L. Efurumibe[b], L.A. Nnanna[b], H.K. Idu[c]

[a] *Department of Physics with Electronics, Evangel University Akaeze, Ebonyi State, Nigeria*
[b] *Department of Physics Michael Okpara University of Agriculture Umudike, Abia State, Nigeria*
[c] *Department of Physics, Taraba State University, Jalingo, Taraba State, Nigeria*

HIGHLIGHTS

- Gamma radiation shielding of baked and unbaked granite bricks were experimentally and theoretically assessed.
- A NaI(Ti) detector and WinXCOM program were used to measure the linear attenuation coefficients.
- Elements composition of samples were analyzed using PIXE spectroscopy.
- The Results show that adding kaolin to granite positively reduced the liquid permeability coefficients.

ABSTRACT

Gamma radiation shielding of baked and unbaked granite bricks produced with 0%, 10%, 20%, 30%, 40%, and 50% of kaolin powder were experimentally and theoretically assessed for possible deployment in liquid radioactive waste storage. A 3 × 3 inches NaI(Ti) detector and WinXCOM program were used to measure the linear attenuation coefficients at different energies. Elements composition of samples were analyzed using particle induced X-ray emission (PIXE) spectroscopy. Results show that adding kaolin to granite positively reduced the liquid permeability coefficients of the bricks but negatively reduced the shielding properties of the bricks. Optimum results were obtained from unbaked sample of granite brick produced with 50% of micro scale kaolin powder (GK50) with mass attenuation coefficient of 0.0663, 0.0572 and 0.0552 $cm^2.g^{-1}$, radiation protection efficiency (RPE) of 38.36%, 34.11% and 33.13% for radiation energies levels of 661.6, 1173.2, and 1332.5 keV respectively and liquid permeability coefficient of 6.53×10^{-11} $m.s^{-1}$. The study concludes that all brick samples were thermally stable, good in gamma radiation shielding and efficient in liquid radioactive waste immobilization.

KEYWORDS

Granite
Kaolin
Gamma shielding
Radioactive waste management
Liquid Permeability

HISTORY

Received: 18 November 2021
Revised: 4 January 2022
Accepted: 12 January 2022
Published: Autumn 2021

1 Introduction

The safe storage and disposal of liquid radioactive wastes and environmental safety around hazardous substances have become an issue of great concern for most researchers in Environmental Engineering. This concern is due to the negative environmental and health implications of these radioactive wastes which produce radiations that are highly hazardous. Considering the wide applications of nuclear technology in many areas of human endeavor, the management and safe storage of wastes generated from these nuclear activities is the key to mitigating the associated risk inherent in the use of these radioactive materials.

The management and safe storage of liquid radioactive wastes involves packaging of these hazardous materials in specially engineered containers for safe storage and disposal. Recently, many methods have been applied in the management and storage of liquid radioactive wastes. These methods include, chemical precipitation, thermal evaporation, ion exchange, sedimentation, physical method and biological methods (Ipek et al., 2002). The process considered in this study involves a physical method of isolating and immobilizing (storing) liquid radioactive wastes with a solid-state engineered storage facility/barrier which must be mechanically and thermochemically stable with relatively high density and low liquid permeability coefficient materials. This physical method of storage considered in this study is highly recommended for developing countries where the technological expertise needed to manage liquid radioactive waste is in short supply.

Liquid radioactive wastes produced from nuclear activ-

*Corresponding author: echeweozoeugene@gmail.com

ities are major sources of hazardous radiations, and among all radiations emitted by radioactive wastes, gamma radiations have over time proved to be the very difficult to shield (Yilmaz, 2011). This is as a result of the higher penetrating power of gamma radiations.

Some materials such as lead (Pb), red mud (bauxite residue), and stainless steel used as barrier for radioactive waste storage are becoming less attractive because of their inherent disadvantages such as toxicity in the case of lead; corrosion and high liquid permeability in the case of red mud (Obaid et al., 2018) and high cost of stainless steel.

Therefore, the need to consider other materials for storage or radioactive wastes cannot be over emphasized. Considering that most radioactive wastes are in liquid form, important criteria for choosing efficient materials for the storage, management and immobilization of liquid radioactive waste are the gamma radiation shielding properties, liquid permeability coefficient, mechanical properties, the thermochemical stability as well as the cost of the material.

Recently, several authors have investigated the radiation shielding capability of different materials (Olukotun et al., 2018; Mann et al., 2016b; Kacal et al., 2019; Najam et al., 2016) without considering the liquid permeabilities coefficients and thermochemical stabilities as well as the cost of these materials. The lack of liquid permeability and thermochemical stability evaluation of any radiation shielding or radioactive storage facilities may result to radioactive waste leakage which has the potential to contaminate the environment and underground water bodies (Kozlowski and Ludynia, 2019; Le et al., 2015).

Among alternative materials which include concrete, kaolin, clay-steel slag, clay-fly ash, bentonite-red mud composites etc are under consideration for effective radiation shielding and storage of radioactive materials (Oto et al., 2013; Echeweozo and Igwesi, 2021; Isfahani et al., 2019b,a; Olukotun et al., 2018; Mann et al., 2016b; Kacal et al., 2019; Najam et al., 2016).

Many current researches have shown granite and clay materials as a naturally, inexpensive materials with high density, thermo-chemical stable, eco-friendly, corrosion resistant, and readily available with excellent results in radiation shielding (Kacal et al., 2019; Galán and Aparicio, 2014; Mann et al., 2016c; Najam et al., 2016). In this study, radiation shielding, liquid permeability properties as well as thermochemical stability of granite bricks produced with different percentage of kaolin powder were investigated for possible deployment in liquid radioactive waste storage and management. The obtained results were also compared with results of other possible alternatives. Generally, the present study investigates the effect of adding granite to kaolin on the radiation shielding properties and thermo-chemical stability of granite-kaolin composites bricks as an environmental engineering strategy for radiation risk mitigation that never been investigated before now.

2 Theoretical Background

At narrow collimated-beam geometry, gamma radiation passing through a shielding material of thickness x(cm) is transmitted according to Beer-Lambert's law:

$$I = I_0\, \mathrm{e}^{-\mu x} \tag{1}$$

where I is the attenuated radiation intensity, I_0 is the initial radiation intensity, μ is the linear attenuation coefficient (LAC), and x is the thickness of material. The mass attenuation coefficient (μ/ρ) is the ratio of the linear attenuation coefficient to the density of the material (Singh et al., 2015). Some important shielding properties are; Half-Value Layer (HVL) and Tenth Value Layer (TVL) which are the thickness of the material reduces the intensity of radiations by a factor of two and ten, respectively.

Also, the Mean Free Path (MFP) is the thickness of material that reduces the original intensity of radiation to 36.8%. The Radiation Protection Efficiency (RPE) which gives the shielding performance of any material in percentage. The RPE values were estimated with Eq. (2) (Singh et al., 2018):

$$\mathrm{RPE} = (1 - \frac{I_x}{I_0}) \times 100 \tag{2}$$

Relative Deviations (RD) between theoretical and experimental MAC [SS1] results were obtained from Eq. (3) (Agar et al., 2019):

$$\mathrm{RD} = \left[\frac{\frac{\mu_{exp}}{\rho} - \frac{\mu_{WinXCom}}{\rho}}{\frac{\mu_{exp}}{\rho}}\right] \times 100 \tag{3}$$

where $\frac{\mu_{exp}}{\rho}$ and $\frac{\mu_{WinXCom}}{\rho}$ are the experimental and theoretical MAC values, respectively.

Liquid permeability coefficient (K) in this aspect measures the ease at which a material allows the flow of radioactive liquids through it. Liquid permeability coefficients of any material can be deduced from the Darcy's formula (Isfahani et al., 2019b). Darcy's formula is expressed as

$$K = \frac{Q\, L\, \Omega}{A\, \Delta h\, t} \tag{4}$$

where Q gives the volume of collected liquid after going through the material (cm^3), t gives the fluid flow time (s), Δh gives change in heights of water pressure (cm), and A gives absorber surface area (cm^2). Also, Ω gives fluid dynamic viscosity (poise or Pa.s) distill water gives 1 poise, L gives absorber's vertical Thickness (cm), and K is the liquid permeability coefficient of the material (darcy or $\mathrm{m.s}^{-1}$)

Experimental and theoretical studies have been carried out to determine radiation shielding properties and liquid permeability of different materials and composites. Isfahani et al. (Isfahani et al., 2019b) determined the liquid permeability and gamma shielding efficiency of clay modified by barite powder using both experimental and simulation methods. In that study, bentonite clay with 10%, 20%, 30%, 40%, 60%, and 80% of barite powder was

prepared to find the optimum percent of barite powder with highest linear attenuation coefficient and lowest liquid permeability coefficient A. The high pure germanium (HPGe) detector was used at gamma energies of 661.6, 1173.2, and 1332.5 keV. They concluded that bentonite clay with 40% of barite is the optimum composition with a permeability factor of 8.879×10^{-11} m.s^{-1} and linear attenuation coefficient of 16.46, 12.2, and 11.99 m^{-1} at gamma energies of 661.6, 1173.2, and 1332.5 keV, respectively.

Agar et al. (Agar et al., 2019) considered shielding properties of Pb/Ag-based alloys in the attenuation of gamma rays. The mass attenuation coefficients (μ/ρ) of these alloys were measured at various gamma energies between 81 to 1333 keV using HPGe detector. They reported that μ/ρ, RPE and HVL for four alloy samples composed of different percentage of Pb and Ag were determined experimentally, theoretically (WinXCom software), and computationally (MCNPX simulation code). The relative deviations between both experimental data (WinXCom) and computational data (MCNPX) values are less than 6% which confirmed that the μ/ρ values were obtained with high accuracy. 75% Pb and 25% Ag alloy sample has the maximum radiation protection efficiency (about 53% at 81 keV). Jawad et al. (Jawad et al., 2019) studied the Radiation shielding properties of some ceramic samples. Eight types of ceramic materials were tested against gamma ray, each type of ceramic modified as glazed and unglazed. The results of the study showed that glazed ceramics are better than unglazed in the attenuation of gamma radiation. Isfahani et al. (Isfahani et al., 2019a) experimentally studied the effect of adding steel slag (industrial wastes) at 10, 20, 30, and 40% mixture to bentonite clay using HPGe detector in order to improve gamma radiation shielding performance at different gamma energies. The results showed that adding steel slag improved the radiation shielding performance of bentonite clay, whereas the mixtures were more permeable to liquid. They noted that 40% steel slag gives the highest gamma radiation shielding coefficient.

Mann et al. (Mann et al., 2016b) experimentally investigated clay fly ash bricks for gamma-ray shielding using NaI(Tl) detector at 661.6, 1173.2, and 1332.5 keV. The clay fly ash bricks showed good shielding properties for moderate energy gamma rays.

Olukotun et al. (Olukotun et al., 2018) studied gamma radiation shielding strength of two clay-materials (Ball clay and kaolin). They employed theoretical and experimental procedures to determine the mass attenuation coefficient, μ/ρ (cm^2.g^{-1}) of clay at gamma energies between 609.31 and 1764.49 keV. A HPGe detector was used for the experiment.

3 Materials and Methods

3.1 Samples

The granite sample used in this research was obtained from Ezillo, quarry site Ebonyi state, Nigeria (5.4155 °N, 7.8586 °E) while kaolin sample was obtained from Umuahia kaolin mining site Abia state, Nigeria (5.5166 °N, 7.4539 °E). The granite specimen was gray, with an average density of 2.68 g.cm^{-3} while the kaolin sample was white with average density of 1.98 g.cm^{-3} (see Table 6).

3.2 Samples Preparation

The samples preparation procedures were carried out as follows: Test samples were pulverized, sun-dried for five days and sieved with 2 μm mesh size. Natural granite (GK00) and granite modified with 10% (GK10), 20% (GK20), 30% (GK30), 40% (GK40), and 50% (GK50) of micro scale kaolin powder were prepared into two parts.

An electronic weighing balance with an accuracy of 0.01 g employed for accurate weighing of the samples. Thereafter, the weighed samples were mixed thoroughly with appropriate amount of distilled water. The samples were then molded and pelletized into small bricks of 3 cm thickness and sun-dried for three days for curing and to remove natural moisture in accordance with American Society for Testing and Material ASTM D6913 (ASTM, 2007; Akande and Agbalajobi, 2013). In all, twelve samples were produced. Six of these samples GK00, GK10, GK20, GK30, GK40, and GK50 were labeled and left to maintain normal lab temperature of 27 °C (unbaked samples). The second part was baked to temperature of 10000 °C for 100 min at a heating rate of 10 °C.min^{-1} using a carbolite muffle furnace and labeled GK00B, GK10B, GK20B, GK30B, GK40B, and GK50B (baked samples). The melting points of all brick samples were determined and recorded alongside their elemental compositions (see Table 6). The elemental composition values determine with Particle or Proton Induced X-ray Emission (PIXE) spectrometry (see Table 6) were imputed in WinXCOM program to determine the theoretical mass attenuation coefficient. This provides comparative analysis of experimental and theoretical results.

3.3 Measurement

3.3.1 Radiation Shielding test

In this work, A 3 × 3 inches NaI(Tl) detector (Canberra Inc. model-802) has been used. The detector system was calibrated for radiation detection in order to accurately converting channel number to energy scale. Gamma spectrometry system was coupled to Gamma Spectacular (model GS-2000 Pro) multichannel analyzer. It was carried out under the same laboratory conditions to mimic as closely as possible, the main experimental conditions. Two radioactive sources [SS1] of three different energy peaks were used to get certain peak at a particular channel number using Cs-137 (energy of 662 keV) and Co-60 (energy of 1170 and 1332 keV). All baked and unbaked samples were subjected to gamma radiation energies of 661.6, 1173.2, and 1332.5 keV.

During the determination of counts, source materials Cs-137 and Co-60 in a lead enclosure with a single face aperture of 6 mm, placed at the back of the source collimator. Samples were irradiated under narrow beam transmission geometry by photons emitted by Cs-137 and Co-60

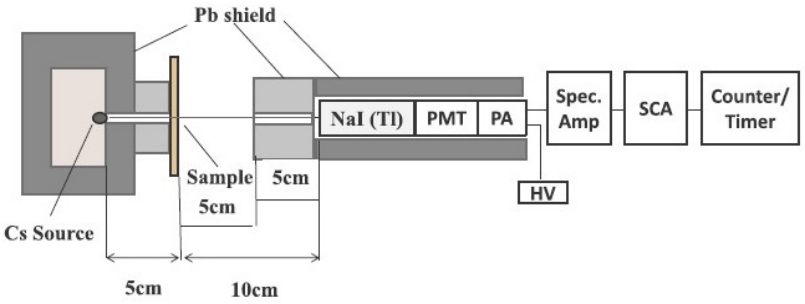

Figure 1: The experimental setup for radiation shielding test.

Table 1: Mass attenuation coefficient and relative deviation for unbaked granite-kaolin composite bricks.

Sample		GK00	GK10	GK20	GK30	GK40	GK50
Density (g.cm^{-3})		2.68	2.65	2.63	2.60	2.58	2.56
MAC for 661.6 keV (cm^2.g^{-1})	Experimental ±5 %	0.0703	0.0694	0.0685	0.0681	0.0674	0.0663
	Theoretical	0.0697	0.0682	0.0679	0.0656	0.0641	0.0631
MAC for 1173.2 keV (cm^2.g^{-1})	Experimental ±5 %	0.0625	0.0615	0.0605	0.0585	0.0579	0.0572
	Theoretical	0.0617	0.0610	0.0570	0.0574	0.0569	0.0572
MAC for 1332.5 keV (cm^2.g^{-1})	Experimental ±5 %	0.0595	0.0584	0.0576	0.0567	0.0559	0.0552
	Theoretical	0.0595	0.0584	0.0565	0.0543	0.0537	0.0547
Relative deviation between experimental and WinXCOM results for various energy levels (%)	661.6 keV	0.74	1.66	0.75	3.64	4.89	4.79
	1173.2 keV	1.34	0.78	4.37	1.83	1.63	0.00
	1332.5 keV	0.00	0.00	1.96	4.18	4.00	0.80

procured from National Institute of Radiation Protection and Research Ibadan (Nigerian Nuclear Regulatory Authority). Counting was accomplished by measuring the spectra of point sources emitting gamma radiations. The transmitted spectra were allowed to record for sufficiently (900 s) to record adequate number of counts under the photopeak, this is to minimize the statistical error. After recording the background counts (I_0), new sample was inserted and a new spectrum recorded and the count rate of area of interest in the photopeak measured for each sample (I). The experimental setup for radiation shielding test is shown in Fig. 1.

The Theremino software (Andrikopoulos et al., 2019) was employed for data acquisition and analysis obtained spectra for I and I_0. Maximum experimental uncertainties of the measured LAC were calculated with the formula for error propagation (Eq. (5)) (Mann et al., 2016a):

$$\Delta\mu = \frac{1}{x}\sqrt{(\frac{\Delta I_0}{I_0})^2 + (\frac{\Delta I}{I})^2 + (\ln\frac{I_0}{I})^2(\frac{\Delta x}{x})^2} \qquad (5)$$

where errors in the values of x, I_0, and I are expressed as Δx, ΔI_0 and ΔI, respectively. The estimated error in the measurement of linear attenuation coefficient was computed. These *errors/uncertainties* were mainly due to counting procedures, thickness measurements, the evaluation of peak areas, and slight deviations from narrow beam geometry in source detector arrangements.

3.3.2 Liquid permeability test

To measure the liquid permeability coefficient of each of the brick samples, a rigid wall permeameter was used. The constant head permeability test procedure was adopted for simplicity. Cylindrical tube/mould with 3.8 cm diameter and 40 cm height were used to measure the liquid permeability coefficient of each of the brick samples. The powdered samples were fried for 15 minutes to eliminate moisture and put in the cylindrical mold and each layer compacted into bricks by 25 drops of the standard hammer in accordance with ASTM D 5856-95 (ASTM, 2007). Initially, the specimen was allowed to be saturated with distil water at very low hydraulic gradient (so as to avoid any compression of air into the voids). After completing the saturation, the measurement for liquid permeability tests was carried out. The water output rate becomes relatively permanent and the system reaches the steady state condition. Therefore, by recording the time 60 s, volume of out coming water flow (Q), change in water pressure height (Δh) and geometry properties of sample such as area (A) and *thickness/Length* of the sample (L), liquid permeability coefficient of the samples (K) by Darcy's law were calculated. Liquid permeability is measured in Darcy (D) or m.s^{-1}, where 1 $D = 0.9869 \times 10^{-12}$ m.s^{-1}. One Darcy is the permeability of a sample 1 cm long with a cross-sectional area of 1 cm^2, when a pressure difference of 1 dyne.cm^{-2} between the ends of the sample causes a fluid with a dynamic viscosity of 1 poise to flow at a rate of 1 cm^3.s^{-1} (Rashid et al., 2015; Echeweozo and Igwesi, 2021; Glover et al., 2006).

4 Results and Discussion

Liquid permeability coefficients and radiation shielding properties (LAC, MAC & RPE) of baked (1000 °C) and unbaked (27 °C) Natural granite (GK00) and granite bricks produced with 10% (GK10), 20% (GK20), 30% (GK30), 40% (GK40), and 50% (GK50) of micro scale kaolin powder were investigated to determine the optimum composition of granite and kaolin composite brick with maximum linear attenuation coefficient and allowable liquid permeability coefficient. The experimental and theoretical mass attenuation coefficients for all the samples at gamma-ray energies of 661.6, 1173.2, and 1332.5 keV for both baked and unbaked composites are reported in Tables 1 and 2, and are graphically shown in Figs. 1 and 2. The mean values of relative deviations (RD) between experimental and theoretical mass attenuation coefficient were computed as 2.75%, 1.66%, and 1.82% for gamma energies of 661.6, 1173.2, and 1332.5 keV, respectively. The low deviation values were within acceptable limit of less than 5% (Agar et al., 2019). This signifies an agreement between experimental and theoretical results. Observed variations in theoretical experimental results could be attributed to source-detector geometry as well as error in mixture rule and density measurements (Medhat and Wang, 2013; Kerur et al., 1992; Akça and Erzeneoğlu, 2014). Therefore, any of these techniques (experimental or theoretical) could be applied independently with reasonable accuracy for the measurement of linear attenuation coefficient and investigation of radiation shielding of materials. RPE, as clearly displayed on Table 3, signifies the shielding abilities of these materials in percentage.

From the results, unbaked samples performed better than baked samples in gamma radiation shielding due to decrease in densities during temperature treatment. The study showed that shielding properties of samples are function of density, thickness of the sample, atomic mass, as well as the energy of the radiation this is in agreement with assertions made by many researchers (Isfahani et al., 2019b,a; Olukotun et al., 2018; Mann et al., 2016b,c; Kacal et al., 2019). It was also observed that MAC of samples decreases as gamma radiation energy increases for both baked and unbaked samples, indicating the strong dependence of MAC on gamma-ray energy. Mass attenuation coefficient is higher for lower energies. The decrease in density observed was mainly caused by a breakdown of interlayer structures (200 °C), loss of zeolite (200 to 300 °C), loss of crystalline (400 °C), and loss of structural water (above 600 °C) in granite and kaolin (Zhang et al., 2016; Qin et al., 2020) and dehydroxylation (loss of hydrogen bonds) and reorientation (resultant phase shift) or the shrinking of kaolin crystal structure which is usually around 20% (Varga, 2007) at temperature above 9500 °C. Although slight cubic expansion was expected during temperature treatment this occurred between 60 °C to 300 °C before slight volume contractions were observed due water loss, dehydroxylation and intra space occupation which is common for granite and kaolin materials (Qin et al., 2020; Yilmaz, 2011; Jaradat et al., 2017; Akande and Agbalajobi, 2013).

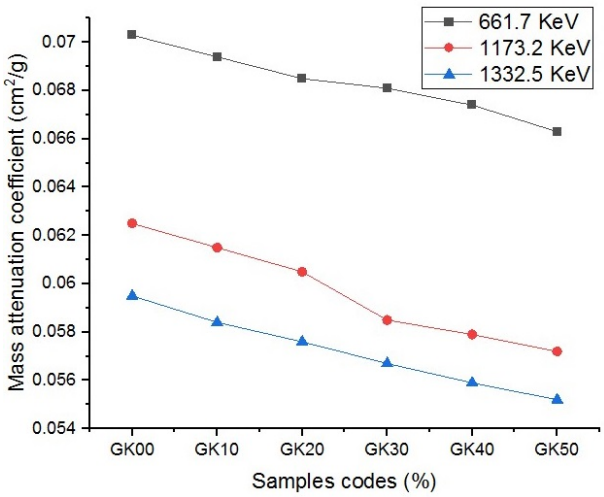

Figure 2: Variation of % mixture against mass attenuation coefficients for unbaked granite-kaolin composite bricks (Experimental results).

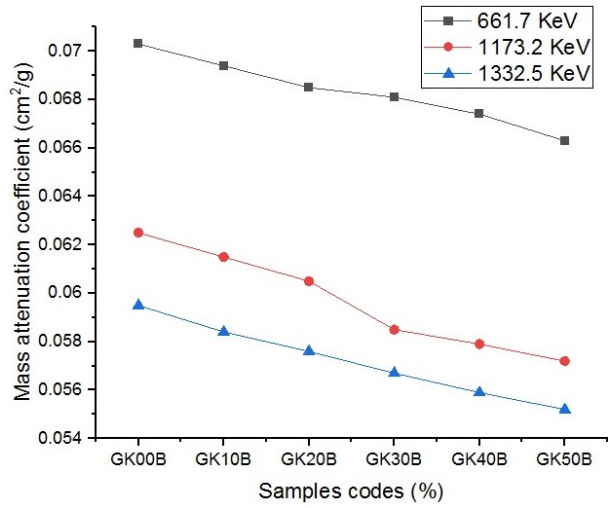

Figure 3: Variation of % mixture against Mass attenuation coefficients for baked granite-kaolin composite bricks (Experimental results).

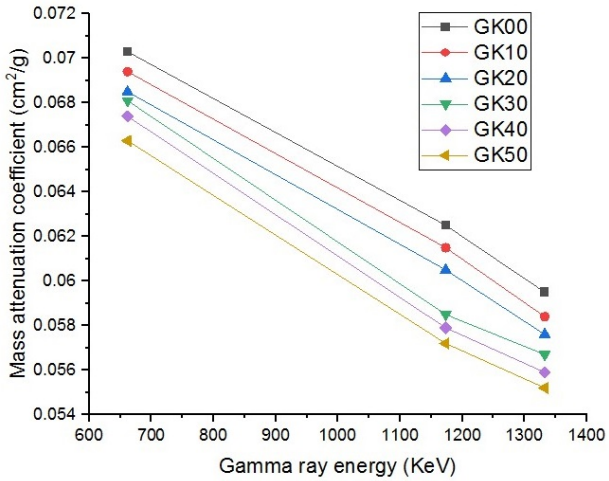

Figure 4: Variation of mass attenuation coefficient with incident energy for different samples of unbaked granite-kaolin composite bricks (Experimental results).

Table 2: Mass attenuation coefficient and relative deviation for baked granite-kaolin composite bricks.

Sample		GK00	GK10	GK20	GK30	GK40	GK50
Density (g.cm^{-3})		2.68	2.65	2.63	2.60	2.58	2.56
MAC for 661.6 keV (cm^2.g^{-1})	Experimental ±5 %	0.0703	0.0690	0.0689	0.0679	0.0673	0.0672
	Theoretical	0.0696	0.0688	0.0680	0.0663	0.0669	0.0649
MAC for 1173.2 keV (cm^2.g^{-1})	Experimental ±5 %	0.0616	0.0616	0.0603	0.0581	0.0577	0.0584
	Theoretical	0.0616	0.0615	0.0595	0.0573	0.5664	0.0581
MAC for 1332.5 keV (cm^2.g^{-1})	Experimental ±5 %	0.0594	0.0581	0.0575	0.0564	0.0557	0.0562
	Theoretical	0.0583	0.0564	0.0562	0.0545	0.0544	0.0545
Relative deviation between experimental and WinXCOM results for various energy levels (%)	661.6 keV	0.91	0.30	1.26	2.31	0.52	3.45
	1173.2 keV	0.00	0.17	0.18	1.39	1.83	0.46
	1332.5 keV	1.83	3.00	1.89	3.41	2.21	3.02

Table 3: Radiation protection efficiency of samples . The last three columns show deviation between baked RPE and unbaked RPE for various energy levels.

Radiation protection efficiency (%) for unbaked samples				Radiation protection efficiency (%) for baked samples				Deviation between baked RPE and unbaked RPE		
Sample code	661.6 keV	1173.2 keV	1332.5 keV	Sample code	661.6 keV	1173.2 keV	1332.5 keV	661.6 keV	1173.2 keV	1332.5 keV
GK00	43.30	39.58	38.15	GK00B	42.60	38.51	37.46	0.70	1.12	0.69
GK10	41.98	38.27	36.76	GK10B	41.37	37.89	36.17	0.61	0.38	0.59
GK20	41.01	37.24	35.87	GK20B	41.00	36.73	35.37	0.01	0.51	0.50
GK30	39.72	34.99	34.14	GK30B	39.20	34.69	33.83	0.52	0.30	0.75
GK40	39.38	34.96	33.98	GK40B	38.79	34.36	33.39	0.59	0.60	0.59
GK50	38.36	34.11	33.13	GK50B	37.82	33.83	32.83	0.54	0.28	0.30

Table 4: Liquid permeability measuring constants/parameters.

Parameter	Value
Time (s)	60
Diameter of sample bed (L) (cm)	3.8
Length of sample bed (L) (cm)	31.5
Area of sample bed (cm^2)	11.34
Temperature (°C)	28.5

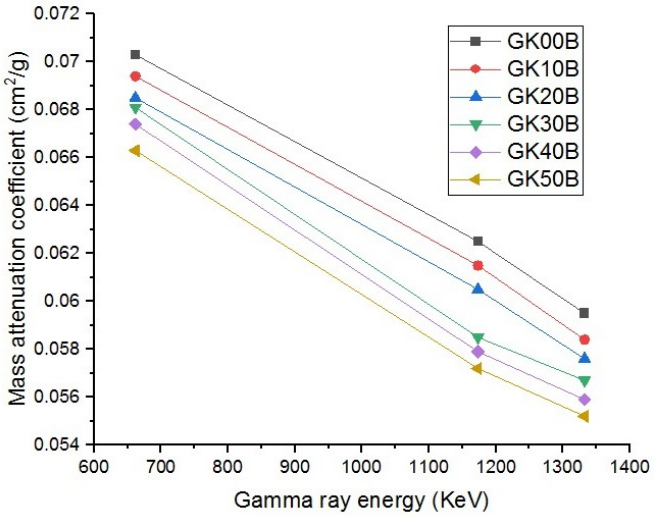

Figure 5: Variation of mass attenuation coefficient with incident energy for different samples of baked granite-kaolin composite bricks (Experimental results).

In this study, melting temperatures of these brick samples were observed between 1334 °C to 1856 °C, at ambient pressure as shown in Table 6. It is important to note that the highest melting point was observed in 50% granite-50% kaolin composite brick with samples code of GK50 which signify high level of thermochemical stability. Considering the melting points of these bricks, granite-kaolin composite bricks have shown to be thermochemically stable to withstand temperature fluctuations which may occur during radioactive waste storage and management. The observed Similarities in results obtained from gamma radiation test of baked and unbaked brick samples shown in Figs. 2 to 5, signify the thermochemically stability of these bricks and by extension their firm mechanical properties enough to withstand environmental fluctuations during radiation shielding and radioactive waste storage procedures.

Tables 4 and 5 about liquid permeability coefficients of all samples show that adding more kaolin to granite increases the liquid permeability coefficients of the samples which is not desirable considering corresponding results obtained from radiation shielding test (Tables 1 and 2).

Liquid permeability coefficient and radiation shielding assessment indicate that increasing the percentage of kaolin powder in granite does not satisfy both maximum linear attenuation coefficient and minimum liquid permeability at the same time. These were clearly shown in Table 7. This was based on the fact that adding kaolin to granite negatively reduces the gamma radiation shielding ability of granite bricks but positively reduces the liquid

Table 5: Liquid permeability test result for granite-kaolin composite bricks.

Sample	(%) of kaolin in Granite	Density ($g.cm^{-3}$)	Water discharged Q (cm^3)	Flow rate ($cm^3.s^{-1}$)	h_1 (mmH_2O)	h_2 (mmH_2O)	Change in water height (mmH_2O)	Liquid permeability (Darcy)	Liquid permeability ($m.s^{-1}$)
GK00	0	2.68	60.89	1.01	236.00	239.98	3.98	40.72	4.03×10^{-11}
GK10	10	2.65	56.15	0.94	232.00	235.84	3.84	43.74	4.32×10^{-11}
GK20	20	2.63	51.30	0.86	242.00	245.69	3.69	49.13	4.58×10^{-11}
GK30	30	2.60	48.89	0.81	224.00	227.48	3.48	55.70	5.50×10^{-11}
GK40	40	2.58	45.13	0.75	232.00	235.21	3.21	61.85	6.10×10^{-11}
GK50	50	2.56	44.01	0.78	234.00	237.07	3.07	66.21	6.53×10^{-11}

Table 6: Element analysis result for unbaked granite-kaolin composite bricks.

Sample Code	KG00	KG10	KG20	KG30	KG40	KG50
Melting point	1334 °C	1796 °C	1812 °C	1827 °C	1844 °C	1856 °C
Element	Element concentration by weight per 1 mg)					
Mg	0.0134	0.0144	0.0168	0.0182	0.0218	0.0230
Al	0.1861	0.2201	0.2421	0.2694	0.2882	0.3014
Si	0.6482	0.5281	0.5101	0.4816	0.3965	0.3241
P	0.0481	0.0366	0.0231	0.0120	0.0084	0.0031
K	0.0245	0.0623	0.0859	0.0894	0.1002	0.1021
Ca	0.0181	0.0198	0.0200	0.0994	0.1038	0.2041
Ti	0.0101	0.0102	0.0096	0.0088	0.0072	0.0041
V	0.00014	0.00004	-	-	-	-
Cr	-	-	-	-	0.0002	0.0002
Mn	0.00024	0.00024	0.00020	0.00018	0.00018	0.00018
Fe	0.0285	0.0224	0.0101	0.0064	0.0046	0.00019
Cu	0.00081	0.0010	0.0014	0.0019	0.0022	0.0024
Zn	0.0052	0.0031	0.0018	-	0.0008	0.00013
Others	0.0166	0.0816	0.0794	0.0127	0.0656	0.03319
TOTAL	1.0000	1.0000	1.0000	1.0000	1.0000	1.0000

permeability coefficients of bricks. This is in line with earlier observations made by Isfahani et al. (Isfahani et al., 2019b) for composites of clay and barite. From literature, the liquid permeability coefficient of every material is determined by factors like; particle size, void ratio of material, nature of absorbed and the liquid, impurity level in the liquid, pressure, Atterberg limit and temperature (Andavan and Varun, 2017). This study has shown that liquid permeability depends on the percentage of kaolin used for each brick as well as density of the brick samples (see Fig. 6). From Table 5 which is graphically presented in Fig. 6, it was further observed that liquid permeability coefficient decreased with increase in density of the bricks. The results obtained from gamma radiation shielding properties and liquid permeability coefficients of granite-kaolin were better when compared with results other gamma radiation shielding alternatives (see Table 7).

Element analysis carried out on all the bricks showed that the major elements in these bricks were silicon, magnesium, aluminum, and potassium (see Table 6) this is in line with assertions made by Chukwu and Ajumiwe (Echeweozo et al., 2021; Tekin et al., 2018). The deep brown coloration of brick samples after temperature treatment were as a result of oxidization of Fe^{2+} ions to Fe^{3+} ions through expulsion oxygen molecules.

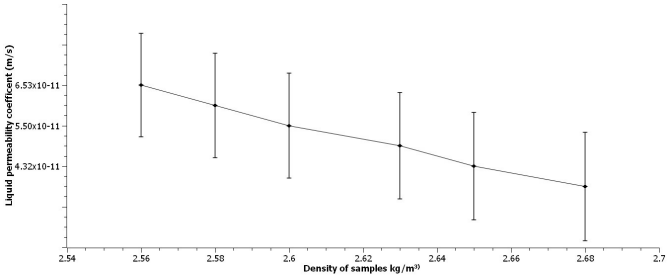

Figure 6: Variation of liquid permeability coefficient against density of brick mixture.

5 Conclusion

In conclusion, granite-kaolin composite bricks as naturally, eco-friendly, inexpensive materials with high density, high thermo-chemical stability, corrosion resistance, and readily available have shown better results in gamma radiation shielding and liquid permeability coefficients. All results obtained from all brick samples were good in radiation shielding with permeability coefficient factors under allowable limit of 10^{-6} to 10^{-14} $m.s^{-1}$ (Ebrahimi-Birang et al., 2004; Fredlund et al., 1994). This makes all unbaked brick samples under consideration a good alternative for liquid radioactive waste immobilization and management.

However, due special consideration to liquid permeability coefficient and thermochemical stability, optimum

Table 7: Comparison of some materials/composites for gamma attenuation and liquid waste immobilization.

Samples with maximum Mass attenuation coefficient	Density ($g.cm^{-3}$)	Linear attenuation coefficient (cm^{-1}) 661.6 keV	1173.2 keV	1332.5 keV	Liquid permeability ($m.s^{-1}$)	References
Clay & 40% barite powder composite	2.55	0.1646	0.1220	0.1199	8.87×10^{-11}	(Isfahani et al., 2019b)
Clay-40% steel slag composite	2.00	0.1587	0.1191	0.1098	3.31×10^{-11}	(Isfahani et al., 2019a)
Baked kaolin (B2)	1.96	-	0.1180	0.1105	-	(Olukotun et al., 2018)
Concrete	2.30	-	0.1366	0.1279	-	(Oto et al., 2013)
Lead (Pb)	11.34	1.0331	0.7258	0.6940	-	(Najam et al., 2016)
Bauxite residue (Red Mud)	2.65	0.2165	0.1590	0.1495	-	(Reddy et al., 2021)
Unbaked kaolin	2.25	0.1656	0.1262	0.1186	2.33×10^{-12}	(Echeweozo and Igwesi, 2021)
Clay-10% fly ash bricks	2.47	0.1364	0.1076	0.1023	-	(Mann et al., 2016b)
Granite100% (GK00)	2.68	0.1885	0.1674	0.1596	4.03×10^{-11}	Present study
Granite-50% Kaolin (GK50)	2.56	0.1698	0.1464	0.1412	6.53×10^{-11}	Present study

results were obtained from unbaked sample of granite brick produced with 50% of micro scale kaolin powder (GK50) with LAC of 0.1698, 0.1464, and 0.1412 cm^{-1}, MAC of 0.0663, 0.0572, and 0.0552 $cm^2.g^{-1}$, RPE of 38.36%, 34.11%, and 33.13% for radiation energies levels of 661.6, 1173.2, and 1332.5 keV, respectively and liquid permeability coefficient of 6.53×10^{-11} $m.s^{-1}$. Therefore, a multilayered exterior wall made of compacted unbaked granite bricks produced with 50% kaolin powder should be deployed in liquid radioactive waste management due its excellent radiation shielding for low energy gamma radiations, its thermochemical stability and good result in liquid radioactive waste immobilization.

References

Agar, O., Sayyed, M., Akman, F., et al. (2019). An extensive investigation on gamma ray shielding features of Pd/Ag-based alloys. *Nuclear Engineering and Technology*, 51(3):853–859.

Akande, J. M. and Agbalajobi, S. A. (2013). Analysis on some physical and chemical properties of Oreke dolomite deposit.

Akça, B. and Erzeneoğlu, S. Z. (2014). The mass attenuation coefficients, electronic, atomic, and molecular cross sections, effective atomic numbers, and electron densities for compounds of some biomedically important elements at 59.5 kev. *Science and Technology of Nuclear Installations*, 2014.

Andavan, S. and Varun, V. (2017). Infiltration, permeability, liquid limit and plastic limit of soil.

Andrikopoulos, C., Zagoraios, G., Mertzimekis, T., et al. (2019). Development of a low–cost γ–ray spectrometry PMT adapter. *HNPS Advances in Nuclear Physics*, 26:235–237.

ASTM (2007). Standard test method for measurement of hydraulic conductivity of porous material using a rigid-wall, compaction-mold permeameter.

Ebrahimi-Birang, N., Gitirana Jr, G., Fredlund, D., et al. (2004). A lower limit for the water permeability coefficient. In *Proceedings of the 57th Canadian Geotechnical Conference, Quebec City. Oct*, pages 24–27.

Echeweozo, E., Asiegbu, A., and Efurumibe, E. (2021). Investigation of kaolin-Granite composite bricks for gamma radiation shielding. *International Journal of Advanced Nuclear Reactor Design and Technology*, 3:194–199.

Echeweozo, E. and Igwesi, D. (2021). Investigation of gamma shielding and liquid permeability properties of kaolin for liquid radioactive waste management. *Applied Radiation and Isotopes*, 176:109908.

Fredlund, D., Xing, A., and Huang, S. (1994). Predicting the permeability function for unsaturated soils using the soil-water characteristic curve. *Canadian Geotechnical Journal*, 31(4):533–546.

Galán, E. and Aparicio, P. (2014). Experimental study on the role of clays as sealing materials in the geological storage of carbon dioxide. *Applied Clay Science*, 87:22–27.

Glover, P., Zadjali, I., and Frew, K. (2006). Permeability prediction from MICP and NMR data using an electrokinetic approach. *Geophysics*, 71(4):F49–F60.

Ipek, U., Öbek, E., Akca, L., et al. (2002). Determination of degradation of radioactivity and its kinetics in aerobic composting. *Bioresource technology*, 84(3):283–286.

Isfahani, H. S., Abtahi, S. M., Roshanzamir, M. A., et al. (2019a). Investigation on gamma-ray shielding and permeability of clay-steel slag mixture. *Bulletin of Engineering Geology and the Environment*, 78(6):4589–4598.

Isfahani, H. S., Abtahi, S. M., Roshanzamir, M. A., et al. (2019b). Permeability and gamma-ray shielding efficiency of clay modified by barite powder. *Geotechnical and Geological Engineering*, 37(2):845–855.

Jaradat, K. A., Darbari, Z., Elbakhshwan, M., et al. (2017). Heating-freezing effects on the orientation of kaolin clay particles. *Applied Clay Science*, 150:163–174.

Jawad, A., Demirkol, N., Gunoğlu, K., et al. (2019). Radiation shielding properties of some ceramic wasted samples. *International Journal of Environmental Science and Technology*, 16(9):5039–5042.

Kacal, M. R., Akman, F., and Sayyed, M. (2019). Investigation of radiation shielding properties for some ceramics. *Radiochimica Acta*, 107(2):179–191.

Kerur, B., Thontadarya, S., and Hanumaiah, B. (1992). A study on the range of non-validity of the Bragg's additivity law for compounds at photon energies below 10 kev. *International Journal of Radiation Applications and Instrumentation. Part A. Applied Radiation and Isotopes*, 43(7):893–898.

Kozlowski, T. and Ludynia, A. (2019). Permeability coefficient of low permeable soils as a single-variable function of soil parameter. *Water*, 11(12):2500.

Le, T. D., Moyne, C., and Murad, M. A. (2015). A three-scale model for ionic solute transport in swelling clays incorporating ion–ion correlation effects. *Advances in Water Resources*, 75:31–52.

Mann, H. S., Brar, G., and Mudahar, G. (2016a). Gamma-ray shielding effectiveness of novel light-weight clay-flyash bricks. *Radiation Physics and Chemistry*, 127:97–101.

Mann, H. S., Brar, G. S., Mann, K. S., et al. (2016b). Experimental investigation of clay fly ash bricks for gamma-ray shielding. *Nuclear Engineering and Technology*, 48(5):1230–1236.

Mann, K. S., Heer, M. S., and Rani, A. (2016c). Investigation of clay bricks for storage facilities of radioactive-wastage. *Applied Clay Science*, 119:249–256.

Medhat, M. and Wang, Y. (2013). Geant4 code for simulation attenuation of gamma rays through scintillation detectors. *Annals of Nuclear Energy*, 62:316–320.

Najam, L. A., Hashim, A. K., Ahmed, H. A., et al. (2016). Study the attenuation coefficient of granite to use it as shields against gamma ray.

Obaid, S. S., Sayyed, M., Gaikwad, D., et al. (2018). Attenuation coefficients and exposure buildup factor of some rocks for gamma ray shielding applications. *Radiation Physics and Chemistry*, 148:86–94.

Olukotun, S., Gbenu, S., Ibitoye, F., et al. (2018). Investigation of gamma radiation shielding capability of two clay materials. *Nuclear Engineering and Technology*, 50(6):957–962.

Oto, B. et al. (2013). Gamma-ray shielding of concretes including magnetite in different rate. *International Journal of Physical Sciences*, 8(8):310–314.

Qin, Y., Tian, H., Xu, N.-X., et al. (2020). Physical and mechanical properties of granite after high-temperature treatment. *Rock Mechanics and Rock Engineering*, 53(1):305–322.

Rashid, F., Glover, P., Lorinczi, P., et al. (2015). Permeability prediction in tight carbonate rocks using capillary pressure measurements. *Marine and Petroleum Geology*, 68:536–550.

Reddy, P. S., Reddy, N. G., Serjun, V. Z., et al. (2021). Properties and assessment of applications of red mud (bauxite residue): current status and research needs. *Waste and Biomass Valorization*, 12:1185–1217.

Singh, K., Singh, S., Dhaliwal, A., et al. (2015). Gamma radiation shielding analysis of lead-flyash concretes. *Applied Radiation and Isotopes*, 95:174–179.

Singh, T., Kaur, A., Sharma, J., et al. (2018). Gamma rays' shielding parameters for some pb-cu binary alloys. *Engineering Science and Technology, An International Journal*, 21(5):1078–1085.

Tekin, H., Erguzel, T., Sayyed, M., et al. (2018). An investigation on shielding properties of different granite samples using MCNPX code. *Digest Journal of Nanomaterials & Biostructures (DJNB)*, 13(2).

Varga, G. (2007). The structure of kaolinite and metakaolinite. *Epitoanyag*, 59(1):6–9.

Yilmaz, G. (2011). The effects of temperature on the characteristics of kaolinite and bentonite. *Scientific Research and Essays*, 6(9):1928–1939.

Zhang, W., Sun, Q., Hao, S., et al. (2016). Experimental study on the variation of physical and mechanical properties of rock after high temperature treatment. *Applied Thermal Engineering*, 98:1297–1304.